Signatures of Majorana fermions in an elliptical quantum ring

Areg Ghazaryan,[1] Aram Manaselyan,[2] and Tapash Chakraborty[1,*]
[1]*Department of Physics and Astronomy, University of Manitoba, Winnipeg, Canada R3T 2N2*
[2]*Department of Solid State Physics, Yerevan State University, Yerevan, Armenia*
(Received 4 February 2016; revised manuscript received 11 April 2016; published 3 June 2016)

We have investigated the signatures of zero-energy Majorana fermions in an anisotropic semiconductor quantum ring that contains a few electrons, has a strong spin-orbit interaction, and proximity coupled to an *s*-wave superconductor. We have found that for rings with sizes of few hundred angstroms and for certain range of values of the chemical potential and an applied magnetic field, the system is very likely in a topological phase with possible indications of the presence of Majorana fermions. In particular, the ground-state energies and the average electron numbers for the states with even and odd electron numbers are almost identical. We have analyzed the wave functions of Majorana fermions in the ring and have shown that Majorana fermions are well separated from each other in the *angular coordinates*. We have also determined the charge-density jumps due to the presence of the Majoranas, that are found to be uniformly distributed along the ring and can perhaps be detected by scanning charge measurements. While a definitive proof of the existence of these exotic particles in a ring has not been provided here, our study indicates the likelihood of the presence of these objects in our chosen system. As the semiconductor quantum rings with a few interacting electrons are available in the laboratories, we believe that the long sought-after Majorana fermions could perhaps be observed in such a system.

DOI: 10.1103/PhysRevB.93.245108

I. INTRODUCTION

Search for Majorana fermions (MFs), the particles that are their own antiparticles [1,2] has intensified in recent years. This is fueled by the possibility to observe the analogs of MFs in condensed matter systems, where they are expected to materialize in the form of zero-energy Majorana quasiparticles [3–5]. These MFs are governed by the non-Abelian exchange statistics. The proposed hybrid semiconductor-superconductor nanostructured systems [4–6] are believed to be the most likely construct hosting such exotic excitations [7], and have naturally received considerable attention by various experimental groups [8–12]. Experimental efforts have also focused on ferromagnetic atomic chains [13] that are in close proximity to a conventional superconductor. A promising route for realization of the MFs [6] is the observation of the topological superconducting phase in a one-dimensional semiconductor quantum wire with large Rashba spin-orbit (SO) coupling [14], proximity coupled to an *s*-wave superconductor. By tuning the chemical potential of the system in the gap region created by an applied magnetic field, the system is effectively rendered spinless and the MFs are expected to reside at the two ends of the wire, akin to Kitaev's original *p*-wave superconductor chain model [15].

Here we show that, semiconductor quantum rings (QR) with their doubly connected geometry and consequent unique quantum properties could perhaps reveal the unique signatures of MFs in such a system. Observation of the Aharonov-Bohm oscillations [16] and the persistent current [17] in small semiconductor QRs, and the recent experimental realization of QRs with only a few electrons [18,19] have made QRs an attractive topic for experimental studies and a unique playground for various many-body effects in these quasi-one-dimensional systems [20]. Although almost circular or slightly oval-shaped QRs have been fabricated by various experimental groups [21–23], anisotropic QRs are the ones most commonly obtained during the growth process [23–26]. Elongated InAs/InP QRs were fabricated by several groups [25,26]. Our studies indicate that an elongated InAs semiconductor QR containing a few electrons, proximity coupled to an *s*-wave superconductor could be an excellent candidate for detecting signatures of MFs since the energy spectrum of this system contains a lot of level crossings due to Aharonov-Bohm oscillations. This periodic energy spectrum for a few interacting electrons entails the suitable conditions required, in particular, with the help of the applied magnetic field we can bring two energy levels with even and odd number parity close to each other thereby facilitating the existence of MFs in such a QR.

II. THEORETICAL FRAMEWORK

In the following, we consider a two-dimensional elliptical QR with strong Rashba SO coupling [14], proximity coupled to an *s*-wave superconductor. In order to model the elliptical ring, we use the procedure outlined previously [27]. In particular, we define the coordinate system in the form $x = ar\cos\theta$, $y = br\sin\theta$, where a and b are constants (which are chosen to have the dimension of length), which define the ellipticity of the QR, while r is the dimensionless radius used to define the size of the QR. We choose the confinement potential of the QR with infinitely high borders: $V_{\rm conf}(r) = 0$, if $R_1 \leqslant r \leqslant R_2$ and infinity otherwise. Clearly, for $a = b$, the QR is circular, while for $a \neq b$, the QR has elliptical boundaries with the eccentricity defined as $\varepsilon = \sqrt{1 - b^2/a^2}$.

In the absence of a superconducting pairing potential, the Hamiltonian of our system is

$$\mathcal{H} = \sum_i^{N_e} \mathcal{H}_{\rm SP}^i + \frac{1}{2}\sum_{i\neq j}^{N_e} V_{ij}, \tag{1}$$

*Tapash.Chakraborty@umanitoba.ca

where N_e is the number of electrons in the QR,

$$V_{ij} = \frac{e^2 e^{-\lambda|\mathbf{r}_i-\mathbf{r}_j|}}{\epsilon|\mathbf{r}_i-\mathbf{r}_j|} \tag{2}$$

is the Yukawa-type screened Coulomb interaction term with screening parameter λ [28], and ϵ is the background dielectric constant. Finally, $\mathcal{H}_{\rm SP}$ is the single-particle Hamiltonian in the presence of an external perpendicular magnetic field and with the SOI included

$$\mathcal{H}_{\rm SP} = H_0 + H_{\rm SO} = \frac{1}{2m_e}\Pi^2 - \mu + V_{\rm conf}(r) + \frac{1}{2}g\mu_{\rm B}B\sigma_z + H_{\rm SO}, \tag{3}$$

where $\Pi = \mathbf{p} + \frac{e}{c}\mathbf{A}$, $\mathbf{A} = B/2(-y,x,0)$ is the vector potential of the applied magnetic field along the z axis in the symmetric gauge, and μ is the chemical potential. The third term on the right-hand side of (3) is the Zeeman splitting. The last term describes the Rashba SOI [14]

$$H_{\rm SO} = \frac{\alpha}{\hbar}[\boldsymbol{\sigma}\times\Pi]_z, \tag{4}$$

with α being the SOI parameter, which depends on the asymmetry in the z direction, generated either by the confinement or by the electric field. We take as basis states the eigenfunctions of H_0 with $B = 0$ when the ring is circular ($a = b$). The eigenfunctions of this Hamiltonian then have the form [29]

$$\phi_{nl}(r,\theta) = \frac{C}{2\pi}e^{il\theta}\left(J_l(\gamma_{nl}r) - \frac{J_l(\gamma_{nl}R_1)}{Y_l(\gamma_{nl}R_1)}Y_l(\gamma_{nl}r)\right) = \frac{1}{2\pi}e^{il\theta}\chi_{nl}(r), \tag{5}$$

where $J_l(r)$ and $Y_l(r)$ are Bessel functions of the first and second kind respectively, $\gamma_{nl} = 2m_e a^2 E_{nl}/\hbar^2$, where E_{nl} are the eigenstates defined from the boundary conditions, and the constant C is determined from the normalization integral $\int_0^{2\pi}\mathrm{d}\theta\int_{R_1}^{R_2}\mathrm{d}r a^2 r|\phi_{nl}(r,\theta)|^2 = 1$. For convenience, we choose the following orthonormal basis states for the elliptical ring:

$$\Phi_{nl}(r,\theta) = \frac{1}{2\pi}\sqrt{\frac{a}{b}}e^{il\theta}\chi_{nl}(r) = \sqrt{\frac{a}{b}}\psi_{nl}(r,\theta), \tag{6}$$

where the $\sqrt{a/b}$ term is included so that the basis states are normalized as $\int_0^{2\pi}\mathrm{d}\theta\int_{R_1}^{R_2} r\mathrm{d}r\, ab|\Phi_{nl}(r,\theta)|^2 = 1$.

The second-quantized form of the many-body Hamiltonian (1) is

$$\mathcal{H} = \sum_{n'l'nl}\left(\sum_s\langle n'l'|H_0|nl\rangle c^\dagger_{n'l's}c_{nls} + \frac{i\alpha}{\hbar}\langle n'l'|\Pi_-|nl\rangle c^\dagger_{n'l'\uparrow}c_{nl\downarrow} - \frac{i\alpha}{\hbar}\langle n'l'|\Pi_+|nl\rangle c^\dagger_{n'l'\downarrow}c_{nl\uparrow}\right) + \frac{1}{2}\sum_{n_1'l_1',n_2'l_2'}\sum_{nl_1,n_2l_2}\sum_{s_1s_2}\langle n_1'l_1',n_2'l_2'|V_{12}|n_1l_1,n_2l_2\rangle \times c^\dagger_{n_1'l_1's_2}c^\dagger_{n_2'l_2's_1}c_{n_1l_1s_1}c_{n_2l_2s_2}, \tag{7}$$

where $c^\dagger_{nls}$ and c_{nls} are creation and annihilation operators and $\Pi_\pm = \Pi_x \pm i\Pi_y$. The nonzero matrix elements for the noninteracting term are (i) for $l' = l$,

$$\langle n'l|H_0|nl\rangle = \frac{E_{nl}}{2}\left(1+\frac{a^2}{b^2}\right)\delta_{n'n} + \frac{\hbar\omega_{\rm B}l}{4}\left(\frac{a}{b}+\frac{b}{a}\right)\delta_{n'n} + \frac{e^2B^2}{16mc^2}(a^2+b^2)\Gamma^{(3)}_{n'l,nl},$$

(ii) for $l' = l+2$,

$$\begin{aligned}\langle n'l'|H_0|nl\rangle &= \frac{E_{nl}}{4}\left(1-\frac{a^2}{b^2}\right)\Gamma^{(1)}_{n'l',nl} - \frac{\hbar^2\gamma_{nl}(l+1)}{4m_e}\left(\frac{1}{a^2}-\frac{1}{b^2}\right)\Lambda^{(0)}_{n'l',nl} + \frac{\hbar\omega_{\rm B}\gamma_{nl}}{8}\left(\frac{a}{b}-\frac{b}{a}\right)\Lambda^{(2)}_{n'l',nl} \\ &\quad + \frac{e^2B^2}{32m_ec^2}(a^2-b^2)\Gamma^{(3)}_{n'l',nl} = \langle nl|H_0|n'l'\rangle,\end{aligned}$$

(iii) for $l' = l+1$,

$$\langle n'l'|\Pi_+|nl\rangle = \frac{i\hbar\gamma_{nl}}{2}\left(\frac{1}{a}+\frac{1}{b}\right)\Lambda^{(1)}_{n'l',nl} + \frac{ieB}{4c}(a+b)\Gamma^{(2)}_{n'l',nl},$$

$$\langle n'l'|\Pi_-|nl\rangle = \frac{i\hbar\gamma_{nl}}{2}\left(\frac{1}{a}-\frac{1}{b}\right)\Lambda^{(1)}_{n'l',nl} - \frac{ieB}{4c}(a-b)\Gamma^{(2)}_{n'l',nl},$$

and (iv) for $l' = l-1$,

$$\begin{aligned}\langle n'l'|\Pi_+|nl\rangle &= i\hbar\left(\frac{\gamma_{nl}}{2}\Lambda^{(1)}_{n'l',nl} - l\Gamma^{(0)}_{n'l',nl}\right)\left(\frac{1}{a}-\frac{1}{b}\right) + \frac{ieB}{4c}(a-b)\Gamma^{(2)}_{n'l',nl}, \\ \langle n'l'|\Pi_-|nl\rangle &= i\hbar\left(\frac{\gamma_{nl}}{2}\Lambda^{(1)}_{n'l',nl} - l\Gamma^{(0)}_{n'l',nl}\right)\left(\frac{1}{a}+\frac{1}{b}\right) - \frac{ieB}{4c}(a+b)\Gamma^{(2)}_{n'l',nl}.\end{aligned}$$

In the above equations $\omega_{\rm B} = eB/m_ec$ is the cyclotron frequency and $\Gamma^{(m)}_{n'l',nl}$ and $\Lambda^{(m)}_{n'l',nl}$ are integrals defined as follows:

$$\Gamma^{(m)}_{n'l',nl} = \int_{R_1}^{R_2} dr a^2 r^m \chi_{n'l'}(r)\chi_{nl}(r), \tag{8}$$

$$\Lambda^{(m)}_{n'l',nl} = \int_{R_1}^{R_2} dr a^2 r^m \chi_{n'l'}(r)K_{nl}(r), \tag{9}$$

where

$$K_{nl}(r) = C(J_{l+1}(\gamma_{nl}r) - J_l(\gamma_{nl}R_1)Y_{l+1}(\gamma_{nl}r)/Y_l(\gamma_{nl}R_1)).$$

In order to evaluate the matrix elements for the Coulomb interaction, we first consider the Fourier transform of the Coulomb potential, which for the case of the Yukawa type

screened potential is $V(\mathbf{k}) = 2\pi e^2/\epsilon\sqrt{\lambda^2 + k^2}$. Then the matrix elements can be written as

$$\langle n_1' l_1', n_2' l_2' | V_{12} | n_1 l_1, n_2 l_2 \rangle = \frac{e^2}{2\pi\epsilon}(-1)^{l_1 - l_2'} \mathrm{i}^{(l_1 + l_2 - l_1' - l_2')} \times \int_0^\infty k\mathrm{d}k \int_0^{2\pi} \mathrm{d}\theta_k \frac{e^{\mathrm{i}(l_1 + l_2 - l_1' - l_2')\theta_k}}{\sqrt{\lambda^2 a^2 b^2 + k^2 b^2 \cos^2\theta_k + k^2 a^2 \sin^2\theta_k}}$$
$$\times \int_{R_1}^{R_2} r_1\, \mathrm{d}r_1 a^2 \chi_{n_1' l_1'}(r_1)\chi_{n_2 l_2}(r_1) J_{l_2 - l_1'}(kr_1) \times \int_{R_1}^{R_2} r_2\, \mathrm{d}r_2 a^2 \chi_{n_2' l_2'}(r_2)\chi_{n_1 l_1}(r_2) J_{l_1 - l_2'}(kr_2). \quad (10)$$

In order to derive the form of the induced superconducting potential for the QR, we start from its general form written with the help of the field operators [5]

$$\mathcal{H}_{\mathrm{SC}} = \int \mathrm{d}^2 r\, \Psi_\downarrow(\mathbf{r})\Delta(\mathbf{r})\Psi_\uparrow(\mathbf{r}) + \mathrm{H.c.}, \quad (11)$$

where for the s-wave superconductor $\Delta(\mathbf{r}) = \Delta e^{-in_\Phi\theta}$ and $n_\Phi = [2\Phi/\Phi_0]$ [30,31]. Here, Δ is real, $\Phi = \pi abR_1^2 B$, $\Phi_0 = hc/e$ and $[v]$ denotes the integer closest to v. By making a transition from the field operators to creation and annihilation operators defined for the basis (6): $\Psi_s(\mathbf{r}) = \sum_{nl} \Phi_{nl}(r,\theta)c_{nls}$, we write the final form for the superconducting potential as

$$\mathcal{H}_{\mathrm{SC}} = \Delta \sum_{n'nl} \Gamma^{(1)}_{n'(n_\Phi - l),nl}[c_{n'(n_\Phi - l)\downarrow} c_{nl\uparrow} + c^\dagger_{n'(n_\Phi - l)\uparrow} c^\dagger_{nl\downarrow}]. \quad (12)$$

In order to evaluate the eigenstates of the total Hamiltonian $\mathcal{H}_{\mathrm{PSC}} = \mathcal{H} + \mathcal{H}_{\mathrm{SC}}$, we use the exact diagonalization procedure to diagonalize $\mathcal{H}_{\mathrm{PSC}}$ in even and odd sectors as reported earlier [28]. For example, for the odd sector, we diagonalize $\mathcal{H}_{\mathrm{PSC}}$ for a system with nonconstant number of electrons, namely $1,3,\ldots,N_e$ electron number basis. A similar procedure is employed for the even sector as well. This gives us the possibility to obtain the low-lying energy states and the wave functions both for even and odd sectors very accurately.

We employ several different approaches to identify the signatures of well separated MFs in the system. In condensed matter systems, isolated MFs are zero-energy quasiparticle excitations and they do not carry a charge [4]. The fermion number parity is a good quantum number. Therefore adding a nonlocal electron which is comprised of two well separated MFs in the system will not alter the total energy or the charge of the system. Even in the case of the system without boundaries where isolated MFs usually reside, the phase transition between the trivial and nontrivial (topological) superconducting states results in closing of the superconducting bulk gap. Based on this premise the first parameter which is used for identifying the phase transition between two superconducting phases and the appearance of isolated MFs is the energy difference between the odd and even sector [32]

$$\Delta E = |E_{\mathrm{odd}} - E_{\mathrm{even}}|. \quad (13)$$

This quantity is expected to vanish in the topological phase but remains finite for the ordinary superconducting state [32]. The next parameter is the charge difference between the even and odd sector ΔN, which is equal to the mean electron number difference between the two sectors. In order to evaluate this parameter, we first calculate the particle densities in each sector

$$\rho_{\mathrm{even,odd}}(\mathbf{r}) = \int d\mathbf{r}_2 d\mathbf{r}_3 \ldots |\Psi_{\mathrm{even,odd}}(\mathbf{r},\mathbf{r}_2,\ldots)|^2, \quad (14)$$

where $\Psi_{\mathrm{even,odd}}(\mathbf{r}_1,\mathbf{r}_2,\ldots)$ is the wave function of the system in the odd and even sector. It is given as a superposition of basis wave functions with different number of electrons up to a maximum number N_e due to the cutoff used in our exact-diagonalization scheme. Clearly, the basis wave function with different number of electrons are orthogonal to each other and the number of integrals in (14) should be taken equal to the number of electrons for each basis state component of $\Psi_{\mathrm{even,odd}}(\mathbf{r}_1,\mathbf{r}_2,\ldots)$ considered as the integrand.

It is known that for a semiconductor quantum wire in the topological superconducting phase, changing the parameters of the system, such as the chemical potential or the magnetic field strength, results in a change of the ground-state parity. For a finite size wire, this is accompanied by a jump of the total electron number and the charge due to the jump is spread along the wire and has an oscillating behavior [33]. Therefore we first calculate the difference between the particle densities in odd and even sector $\Delta\rho(\mathbf{r}) = \rho_{\mathrm{odd}}(\mathbf{r}) - \rho_{\mathrm{even}}(\mathbf{r})$ and compare our results for the ring with what one expects in a quantum wire [33]. The charge difference between the odd and even sector ΔN is the cumulative difference between the particle densities, i.e., $\Delta N = \int d\mathbf{r}\Delta\rho(\mathbf{r})$. Finally, we also calculate the MF probability distributions directly using the procedure outlined previously [28,32]

$$p^{(j)}(r,\theta) = \sum_s \left| \sum_{nl} d^{(j)}_{nls} \Phi^*_{nl}(r,\theta) \right|^2, \quad (15)$$

where $d^{(j)}_{nls}$ are the expansion coefficients of the linear expansion of the MFs operators γ_a in terms of the electron creation and annihilation operators $c^\dagger_{nls}$ and c_{nls}. Here, $j = 1$ and $j = 2$ correspond to two Majorana states which are the constituents of the nonlocal electron.

III. RESULTS AND DISCUSSION

For our present work, we consider the InAs semiconductor QR with parameters: $m_e = 0.042m_0$, where m_0 is the bare electron mass, $g = -14$, $\epsilon = 14.6$ [34], and the SO coupling strength $\alpha = 20$ meV nm [35]. We take the superconducting pairing potential strength to be $\Delta = 0.225$ meV and consider the cases when $n_\Phi = [2\Phi/\Phi_0]$ or $n_\Phi = 0$. As for the ring geometry parameters, we take $R_1 = 3$ and $R_2 = 8$, $a = 10$ nm. For b, we have used two values $b = 6$ and 8 nm, which correspond to values of eccentricities of the elliptical boundaries $\varepsilon = 0.8$ and 0.6, respectively. In what follows, we disregard the interaction between electrons, which means that we take $\lambda = \infty$. The role of interaction in our scheme will be addressed below.

In Fig. 1, the magnetic field dependence of the low-lying states are presented for a single electron in an elliptical QR for

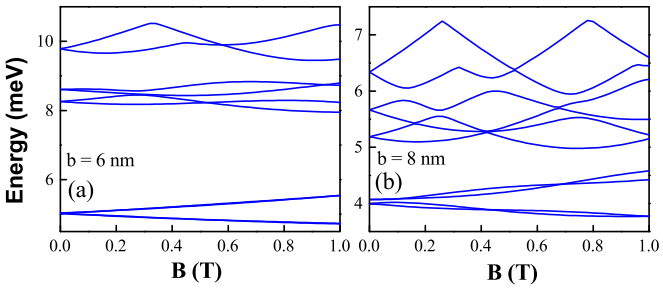

FIG. 1. The dependence of the low-lying energy states on magnetic field B for a single electron in an elliptical quantum ring for (a) $b = 6$ nm and (b) $b = 8$ nm. Chemical potential is chosen to be $\mu = 0$.

$b = 6$ nm (a) and $b = 8$ nm (b). Reduction of the symmetry of the ring from circular to C_2 due to ellipticity results in a separation of the low-lying two energy states (for each spin component) from the other states. This can be clearly seen in Fig. 1, where four energy levels are separated from the higher excited states by more than 1 meV. For $b = 6$ nm, the two states for each spin direction are so close to each other that they cannot be distinguished in the Fig. 1(a). Further, the Aharonov-Bohm oscillations are observed both for the low-lying group of states and also for higher excited states. It should be noted that observation of Aharonov-Bohm oscillations for the low-lying states means that there is a finite probability for electrons to transfer from one side of major axis of the QR to the other. As will be shown below, this is essential for confining two MFs of the nonlocal electron at the two sides. For consideration of the topological phase, we will tune the chemical potential in the energy range of the low-lying quadruplet. Due to the fact that $\Delta < 1$ meV, we can limit the maximum number of electrons to four. Therefore for the odd sector we will consider the number of electrons to be one or three. For the even sector, considering the system size up to four electrons, results in a Hilbert space size bigger than 700 000, which makes the calculation of the energy levels quite challenging. In order to make the Hilbert space smaller for the even sector, we will take the number of electrons to be zero or two. This approximation is valid only when the separation between the two doublets in the quadruplet is comparable to Δ, which is true for $B > 0.3$ T.

In Fig. 2, the dependence of the ground-state energies for the even and the odd sector is shown as a function of (a) the magnetic field B and (b) the chemical potential μ.

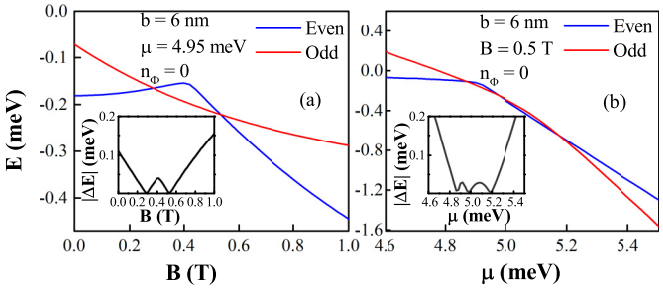

FIG. 2. The dependence of the energies of the ground states of odd and even sector on the magnetic field B (a) and the chemical potential μ (b). Insets show the absolute difference between the energies of the ground states. The ring parameter is $b = 6$ nm and $n_\Phi = 0$.

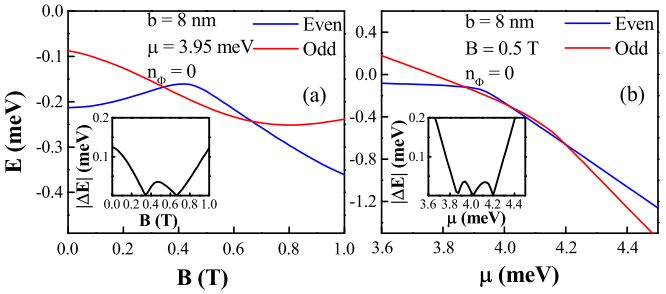

FIG. 3. Same as in Fig. 2 but for $b = 8$ nm.

The ring parameter b is taken to be equal to 6 nm and the superconducting phase $n_\Phi = 0$. Insets show the absolute energy difference for the same ranges. As can be seen from Fig. 2(a) for the magnetic field range $B = 0.28$–0.55 T, the two ground states come close to each other and the energy difference is less than 0.05 meV. In a quantum wire proximity coupled to an s-wave superconductor, the wire is in the topological phase above certain threshold values of the magnetic field ($V_Z > \sqrt{\mu^2 + \Delta^2}$, where V_Z is the Zeeman energy) and remains so, as long as the magnetic field is not strong enough to suppress s-wave pairing due to the spin alignment. That is not the case here for the QR, because the orbital effects and the Aharonov-Bohm oscillations play a substantial role and push the states far from each other after a certain magnetic field. Therefore, for a QR, we get only a range of about 0.3 T when the QR is in the topological state. Although Fig. 2 corresponds to the case when $n_\Phi = 0$, considering $n_\Phi = [2\Phi/\Phi_0]$ does not have any effect on the results for $b = 6$ nm, because in this case $[2\Phi/\Phi_0] = 0$ up to $B = 0.6$ T. A similar feature of the odd and even ground states being close to each other is observed also for the dependence on μ and is depicted in Fig. 2(b). The range of the topological phase spans from $\mu = 4.85$ to 5.2 meV. There is a crossing inside this range between the ground-state energies of the two sectors and therefore the absolute energy difference shows oscillatory behavior.

In Fig. 3, the same dependence is shown as in Fig. 2 but for the ring parameter $b = 8$ nm. As can be seen from Fig. 3, similar patterns are observed for the ground states in the even and odd sectors, just as for $b = 6$ nm. The magnetic field range where the two ground states come close to each other is slightly shifted to higher magnetic fields, namely $B = 0.34$–0.66 T, but the range remains almost the same. The same is also true for the chemical potential range, although that range is shifted by 1 meV to the smaller values, which is the consequence of the single-particle energy difference between $b = 6$ nm and $b = 8$ nm as is shown in Fig. 1. This confirms that the obtained results for the odd and even ground states coming close to each other is not accidental, or only for the choice of $b = 6$ nm, but rather a clear indication of the topological phase which is universal for the anisotropic QR. This will result in the observation of confined MFs inside the topological phase region, as will be shown below. The same dependencies as in Fig. 3, but for $n_\Phi = [2\Phi/\Phi_0]$ are shown in Fig. 4. As can be seen from the results for $b = 8$ nm, the transition between $n_\Phi = 0$ and $n_\Phi = 1$ takes place in the topological phase region and this has a detrimental effect on the robustness of the

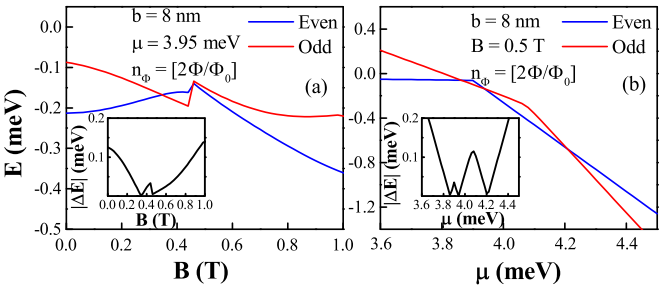

FIG. 4. Same as in Fig. 2 but for $b = 8$ nm and $n_\Phi = [2\Phi/\Phi_0]$.

topological phase or the extent of confinement of the MFs. For the magnetic field dependence, the topological phase range is about 0.12 T and is considerably reduced compared to the case of $n_\Phi = 0$. As for the chemical potential dependence, while the range where even and odd ground states come close to each other is the same as for $n_\Phi = 0$, the absolute difference between the energies is considerably higher and reaches up to 0.1 meV for $\mu = 4.1$ meV. This is a clear indication of the increase of the overlap between two MFs confined at the two sides of the major axis of the QR.

In order to confirm that the pattern observed above is related to the phase transition between nontopological and topological phases in Fig. 5, we present the dependence of the difference between the first excited and the ground-state energies (ΔE) of the odd and even sectors on the magnetic field B and (a) the chemical potential μ (b), for the ring parameter $b = 8$ nm and the superconducting phase $n_\Phi = 0$. As for the magnetic field dependence of ΔE, there is a minimum at $B = 0.44$ T for the even sector and $B = 1$ T for the odd sector. The difference is exactly zero for the odd sector at the minimum, whereas it is 0.05 meV for the even sector. These locations where the minima occur correspond to the closing of the superconducting bulk gap. They are slightly shifted from the positions where the ground states in the even and odd sectors come close to each other and cross. This discrepancy and also the result that for the even sector ΔE is not exactly zero can be attributed to the computational limitations of our exact-diagonalization scheme in obtaining the excited state energies with desired accuracy because of the cutoff in the basis states necessarily used in the calculation. In Fig. 5(b), similar results are observed for the chemical potential (μ) dependence. The minima appear at $\mu = 3.92$ meV for the even sector and at $\mu = 4.16$ meV for

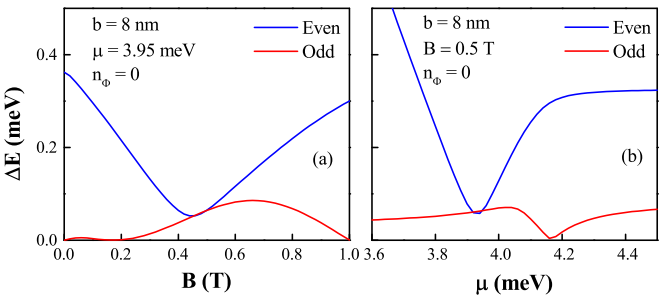

FIG. 5. The difference between the first excited and the ground state energies of odd and even sector vs the magnetic field B (a) and the chemical potential μ (b). The ring parameter is $b = 8$ nm and $n_\Phi = 0$.

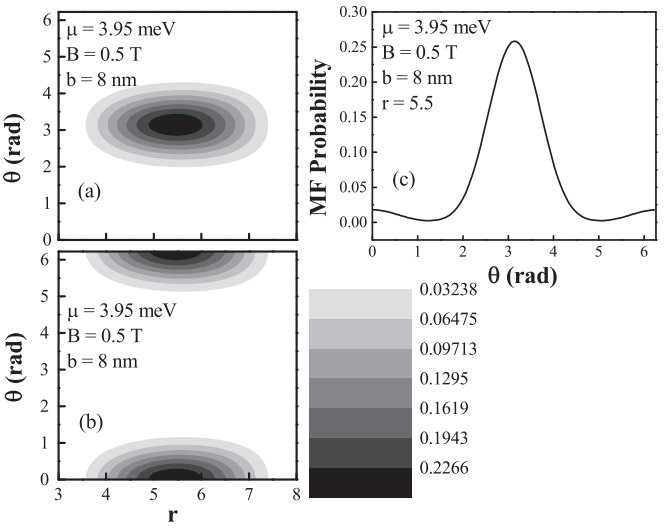

FIG. 6. The MF probability distribution inside the ring for $B = 0.5$ T, $\mu = 3.95$ meV, and for ring parameter $b = 8$ nm. In (a) and (b), we show the contour plots of the MF probability distribution for the MF(1) and MF(2) as defined by (15). (c) The dependence of MF probability distribution on angle θ for MF(1) and $r = 5.5$. In all figures, $n_\Phi = 0$.

the odd sector. Although the minimum of ΔE for the even sector is again around 0.05 meV, the locations of the minimum are in better agreement with the crossing points observed in Fig. 3(b). This is perhaps an additional indication that the observed pattern of even and odd sector ground-state energies being close to each other is likely related to the topological and nontopological phase transition in the system.

Further support for the existence of confined MFs in our QR comes from the MF probability distribution [as defined by (15)] in Figs. 6(a) and 6(b) with $b = 8$ nm, $B = 0.5$ T, and $\mu = 3.95$ meV. Here the contour plots of the MF probability distribution are shown for MF(1) and MF(2). Clearly, each MFs are located at one side of the major axis of the QR. In particular, MF(1) is confined in the location of the QR with $\theta = \pi$ and MF(2) in location with $\theta = 0$, while both MFs are mostly confined in the center of the QR along the r direction. Similar distribution is also observed for $b = 6$ nm. In Fig. 6(c), the dependence of the MF distribution on the angle θ is shown for MF(1) and $r = 5.5$ (this corresponds to the center of the QR in the r direction). The MF distribution has a Gaussian form and the probability of the MF(1) on the other side of the major axis of the QR is considerably smaller than at the side where it is mostly confined. The reason why a QR with sizes of a few hundred angstrom is enough to localize the MFs is that the infinite central barrier of the QR prevents a direct overlap of the MFs. The only way the MFs can overlap would be through two narrow strips that connect the two sides of the major axis of the QR. This property is only present in a QR and not in other low-dimensional systems, such as the quantum wires or quantum dots [36]. By changing the value of the parameter b away from that of a, the transfer amplitude between the two sides of the QR can be controlled. Further, confined MFs appear only at the major axis of the QR, which means that the direction at which the QR is elongated defines where the MFs will likely be confined. Therefore it is important to note that in

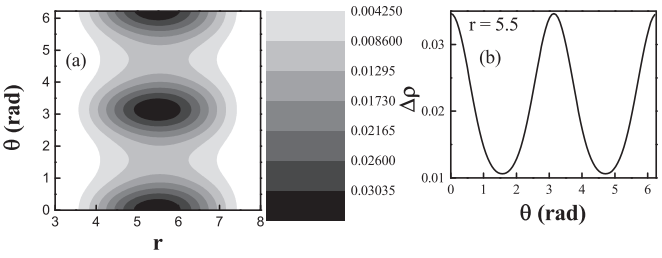

FIG. 7. (a) Contour plot of the difference between the single-particle densities of the many-body states in odd and even sector for $b = 8$ nm. The parameters are $B = 0.5$ T, $n_\Phi = 0$, and $\mu = 3.95$ meV. (b) The dependence of the difference between the single-particle densities on the angle θ for $r = 5.5$ and for the same parameters as in (a).

a QR, both the position of the MFs and the extent by which they are confined can be controlled by external means. This is an important outcome for moving the Majoranas along the ring.

Finally, in Fig. 7(a), the contour plot of the difference between the single-particle densities of the many-body states in odd and even sectors is presented for a QR with $b = 8$ nm. The magnetic field is $B = 0.5$ T and the chemical potential is $\mu = 3.95$ meV. The dependence of the same single-particle densities on angle θ for $r = 5.5$ is presented in Fig. 7(b). We have calculated the mean electron number difference for these parameter values and have found that $\Delta N = 0.32$. The mean electron number difference being less than one indicates once more that the MFs of the nonlocal fermion are confined at the two sides of the major axis of the QR. Figure 7 shows how this charge difference is distributed in the ring. In fact, these two figures indicate that it is mostly confined in the center part of the ring in the r direction but is spread through the whole ring in the θ direction and has the oscillatory behavior with maxima at the two sides of the QR. This result is in accord with the result for a semiconductor wire [33], and as proposed in case of the wire it can be used in the single-electron transistor measurement as an indication of the topological phase and confined MFs.

We have also done similar studies with the Coulomb interaction included. As was noted earlier [28], some screening is essential for the stability of the topological phase. Therefore we have done the calculations using the screening parameter value $\lambda = 0.1\,\text{nm}^{-1}$. While a detailed study of the complete phase diagram is needed to understand the comprehensive effect of interaction on the obtained results, our results for some points in the diagram indicate that in most cases the interaction does not, in any way, improve either the stability of the topological phase or confinement of the MFs in a QR. Therefore superconducting materials with high level of screening for electrons in the semiconductor QR will perhaps be most suitable for detecting the Majoranas.

In conclusion, we have studied here the electronic states in a few-electron semiconductor quantum ring with a strong SOI and proximity coupled to an s-wave superconductor. Although we have not proven rigorously the existence of MFs in a quantum ring, our present study indicates the likelihood of the presence of MF states in such a system. We have shown that for the ranges of the chemical potential and the magnetic field considered here, the difference between the ground-state energies of even and odd electron number system is close to zero and has the oscillatory behavior. This observation is not specific to special ring parameters as was shown by considering two anisotropic quantum rings with elliptical barriers and different eccentricities. From the Majorana fermion probability distribution, we have shown that the Majorana fermions could be located at the two sides of the major axis of the quantum ring. Both the position and the extent of the MF confinement can be controlled externally by choosing the direction of elongation and the eccentricity of the elliptical barriers. Due to these reasons, we believe that few-electron quantum rings are perhaps appropriate for locating the MFs. Optical spectroscopy [18] or magnetotransport measurements [19] of quantum rings are known to provide important information on the energy spectrum that will be crucial in determining the appropriate ΔE and ΔN. Observation of various important properties discussed above, such as the MF probability distribution, charge jumping, etc., would establish the MF signatures in a quantum ring. There were some theoretical studies of Majorana fermions and topological phase transitions in "superconducting" rings [30,31,37,38], and various other ring configurations [39]. However, finding appropriate materials in these cases would be a major challenge. On the other hand, semiconductor quantum rings containing a few electrons are in fact, available in the laboratories, and we believe that signatures of Majorana fermions can perhaps be observed in such a system. Interestingly, it is also possible to envision adiabatic manipulations of the MFs in a quantum ring without resorting to any complicated networks as is essential in a quantum wire [40].

ACKNOWLEDGMENTS

The work has been supported by the Canada Research Chairs Program of the Government of Canada and by the Armenian State Committee of Science Research grant (Project No. 13YR- 1C0014). One of us (T.C.) would like to thank Rolf Haug (Hannover) for very useful discussions on semiconductor quantum rings.

[1] E. Majorana, Nuovo Cimento **14**, 171 (1937).
[2] F. Wilczek, Nat. Phys. **5**, 614 (2009).
[3] In what follows, we use the term Majorana fermions to mean the zero-energy Majorana quasiparticles in condensed matter systems.
[4] J. Alicea, Rep. Prog. Phys. **75**, 076501 (2012).
[5] M. Leijnse and K. Flensberg, Semicond. Sci. Technol. **27**, 124003 (2012).
[6] R. M. Lutchyn, J. D. Sau, and S. Das Sarma, Phys. Rev. Lett. **105**, 077001 (2010); Y. Oreg, G. Refael, and F. von Oppen, *ibid.* **105**, 177002 (2010).
[7] Other possibilities include the Pfaffian states in the fractional quantum Hall effect that can carry the zero energy Majorana fermions [N. Read and D. Green, Phys. Rev. B **61**, 10267 (2000); G. Moore and N. Read, Nucl. Phys. B **360**, 362 (1991)]; See also, T. Chakraborty and V. Apalkov, in *Physics of Graphene*, edited

by H. Aoki and M. S. Dresselhaus (Springer, New York, 2014), Chap. 8; V. M. Apalkov and T. Chakraborty, Phys. Rev. Lett. **107**, 186803 (2011); **97**, 126801 (2006); **105**, 036801 (2010).

[8] V. Mourik, K. Zuo, S. M. Frolov, S. R. Plissard, E. P. A. M. Bakkers, and L. P. Kouwenhoven, Science **336**, 1003 (2012).

[9] M. T. Deng, C. L. Yu, G. Y. Huang, M. Larsson, P. Caroff, and H. Q. Xu, Nano Lett. **12**, 6414 (2012).

[10] A. Das, Y. Ronen, Y. Most, Y. Oreg, M. Heiblum, and H. Shtrikman, Nat. Phys. **8**, 887 (2012).

[11] H. O. H. Churchill, V. Fatemi, K. Grove-Rasmussen, M. T. Deng, P. Caroff, H. Q. Xu, and C. M. Marcus, Phys. Rev. B **87**, 241401 (2013).

[12] M. T. Deng, C. L. Yu, G. Y. Huang, M. Larsson, P. Caroff, and H. Q. Xu, Sci. Rep. **4**, 7261 (2014).

[13] S. Nadj-Perge, I. K. Drozdov, J. Li, H. Chen, S. Jeon, J. Seo, A. H. MacDonald, B. A. Bernevig, and A. Yazdani, Science **346**, 602 (2014).

[14] Y. A. Bychkov and E. I. Rashba, J. Phys. C **17**, 6039 (1984).

[15] A. Y. Kitaev, Phys. Usp. **44**, 131 (2001).

[16] Y. Aharonov and D. Bohm, Phys. Rev. **115**, 485 (1959).

[17] M. Büttiker, Y. Imry, and R. Landauer, Phys. Lett. A **96**, 365 (1983).

[18] A. Lorke, R. J. Luyken, A. O. Govorov, J. P. Kotthaus, J. M. Garcia, and P. M. Petroff, Phys. Rev. Lett. **84**, 2223 (2000).

[19] U. F. Keyser, C. Fühner, S. Borck, R. J. Haug, M. Bichler, G. Abstreiter, and W. Wegscheider, Phys. Rev. Lett. **90**, 196601 (2003); A. Fuhrer, S. Lüscher, T. Ihn, T. Heinzel1, K. Ensslin, W. Wegscheider, and M. Bichler, Nature (London) **413**, 822 (2001).

[20] T. Chakraborty, Adv. Solid State Phys. **43**, 79 (2003); D. S. L Abergel, V. M. Apalkov, and T. Chakraborty, Phys. Rev. B **78**, 193405 (2008); S. Viefers, P. Koskinen, P. Singha Deo, M. Manninen, Physica E **21**, 1 (2004); P. Pietiläinen and T. Chakraborty, Solid State Commun. **87**, 809 (1993); K. Niemelä, P. Pietiläinen, P. Hyvönen, and T. Chakraborty, Europhys. Lett. **36**, 533 (1996); T. Chakraborty and P. Pietiläinen, Phys. Rev. B **50**, 8460 (1994).

[21] *Physics of Quantum Rings*, edited by V. M. Fomin (Springer-Verlag, Berlin Heidelberg, 2014).

[22] R. Blossey and A. Lorke, Phys. Rev. E **65**, 021603 (2002).

[23] P. Offermans, P. M. Koenraad, J. H. Wolter, D. Granados, J. M. Garcia, V. M. Fomin, V. N. Gladilin, and J. T. Devreese, Appl. Phys. Lett. **87**, 131902 (2005).

[24] J. Wu, Z. M. Wang, K. Holmes, E. Marega, Jr., Z. Zhou, H. Li, Y. I. Mazur, and G. J. Salamo, Appl. Phys. Lett. **100**, 203117 (2012).

[25] T. Raz, D. Ritter, and G. Bahir, Appl. Phys. Lett. **82**, 1706 (2003).

[26] J. Sormunen, J. Riikonen, M. Mattila, J. Tiilikainen, M. Sopanen, and H. Lipsanen, Nano. Lett. **5**, 1541 (2005).

[27] D. Berman, O. Entin-Wohlman, and M. Ya. Azbel, Phys. Rev. B **42**, 9299 (1990).

[28] A. Ghazaryan and T. Chakraborty, Phys. Rev. B **92**, 115138 (2015).

[29] A. Ghazaryan, A. Manaselyan, and T. Chakraborty, Physica E **66**, 157 (2015).

[30] F. Pientka, A. Romito, M. Duckheim, Y. Oreg, and F. Oppen, New J. Phys. **15**, 025001 (2013).

[31] B. Scharf and I. Žutić, Phys. Rev. B **91**, 144505 (2015).

[32] E. M. Stoudenmire, J. Alicea, O. A. Starykh, and M. P. A. Fisher, Phys. Rev. B **84**, 014503 (2011).

[33] G. Ben-Shach, A. Haim, I. Appelbaum, Y. Oreg, A. Yacoby, and B. I. Halperin, Phys. Rev. B **91**, 045403 (2015).

[34] T. Chakraborty and P. Pietiläinen, Phys. Rev. Lett. **95**, 136603 (2005); P. Pietiläinen and T. Chakraborty, Phys. Rev. B **73**, 155315 (2006).

[35] C. Fasth, A. Fuhrer, L. Samuelson, V. N. Golovach, and D. Loss, Phys. Rev. Lett. **98**, 266801 (2007).

[36] P. A. Maksym and T. Chakraborty, Phys. Rev. Lett. **65**, 108 (1990); T. Chakraborty, *Quantum Dots: A Survey of the Properties of Artificial Atoms* (Elsevier, New York, 1999).

[37] B. Rosenstein, I. Shapiro, and Ya. Shapiro, Europhys. Lett. **102**, 57002 (2013).

[38] M. Lee, H. Khim, and M. S. Choi, Phys. Rev. B **89**, 035309 (2014).

[39] Ph. Jacquod and M. Büttiker, Phys. Rev. B **88**, 241409 (2013); W.-J. Gong, Y. Zhao, Z. Gao, G. Yi, and X. Zhang, J. Phys. Soc. Jpn. **84**, 024707 (2015); E. Grosfeld and A. Stern, Proc. Natl. Acad. Sci. U.S.A. **108**, 11810 (2011).

[40] B. I. Halperin, Y. Oreg, A. Stern, G. Refael, J. Alicea, F. von Oppen, Phys. Rev. B **85**, 144501 (2012); D. J. Clarke, J. D. Sau, and S. Tewari, *ibid.* **84**, 035120 (2011).